A STUDY OF THE NUCLEAR QUADRUPOLE RESONANCE SPECTRUM OF BERYLLIUM IN CHRYSOBERYL

by

Harry Lee Reaves

Dissertation submitted to the Graduate Faculty of
the Virginia Polytechnic Institute
in candidacy for the degree of
DOCTOR OF PHILOSOPHY
in
Physics

April 1963

Blacksburg, Virginia

TABLE OF CONTENTS

LIST OF FIGURES

I. INTRODUCTION

In 1945 Purcell, Torrey, and Pound (11) and independently Bloch, Hansen, and Packard (2) discovered that certain nuclei, in macroscopic amounts, if placed in a steady magnetic field can be made to interact with an oscillating magnetic field. Both groups observed the proton resonance, the first in a paraffin sample, the second in a water sample. The sample was placed in a steady magnetic field in order that the protons can align with respect to the steady field, H_o. There can be only two possible positions for the protons with an energy difference between the positions of $2\mu H_o$, where μ is the magnetic moment of the proton. Transitions from the lower level to the higher level can be observed if an oscillating magnetic field of resonant frequency $2\mu H_o/h$ is applied to the sample perpendicular to the steady field.

This discovery, known as nuclear magnetic resonance, and the experimental techniques that have developed, are applied in many different scientific fields. Andrew (1, p.5) mentioned that by 1954 over 400 publications had already appeared. There are a number of good articles that review the theory and applications of nuclear magnetic resonance in physics and chemistry (1) (9) (6). In the particular field of crystal structure Cohen and Reif (4, p. 398)

give the various nuclei and crystals that have been studied prior to 1957.

Nuclei that in addition to a magnetic moment also possess an electric quadrupole moment can interact electrically with their environment. Depending on the strength of the magnetic field this interaction can be quite large or quite small in comparison to the magnetic interaction. Dehmelt and Krüger (1, p. 216) in 1950 first investigated the former or "low field" case as it is called. Pound (10) in the same year studied the latter or "high field" case. He developed the theory for the quadrupole interactions in single crystals with axially symmetric field gradients at the nuclear sites. He then verified his theory in a number of excellent experiments on different nuclei in several different types of single crystals.

Volkoff, Petch, and Smellie (17) extended Pound's theory to include the case of an asymmetric field gradient at the nuclear site. They developed a method for determining the orientation of the principal axes of the electric field gradient from an analysis of the change in the frequency of the absorption lines in the nuclear magnetic resonance spectrum as the crystal is rotated perpendicular to the magnetic field. They then applied their method to the Li^7 site in a single crystal of spodumene. A number of sites in various crystals have been investigated in

this manner. The aluminum sites in chrysoberyl have been studied by Hockenberry, Brown, and Williams (8).

It is the purpose of this thesis to apply this Volkoff method to the beryllium nuclei in a single crystal of chrysoberyl. The crystal has been rotated about three mutually perpendicular axes and the rotation pattern for each has been obtained. An analysis of these patterns has given the orientation of the principal axes, the asymmetry parameter, and the quadrupole coupling constant for these beryllium sites. Section II contains the theory of the interaction of a nucleus with its electric environment and develops the equations for the observed quadrupole effects. The method used to analyze the observations and the chrysoberyl structure is also discussed. Section III discusses the equipment that is used and the method of obtaining the data. Section IV gives the interpretation of the data and the conclusions that are drawn from the data.

II. REVIEW OF LITERATURE

A. Nuclear Electric Quadrupole Interaction

Cohen and Reif (4,p.326) developed the electric quadrupole interaction in quite some detail. The following account is a brief review of their development.

Consider a nucleus with a charge density $\rho(\vec{x})$ at the point $\vec{x}$ and whose total charge Ze is distributed over the nuclear volume. Let $\phi(\vec{x})$ be the electrostatic potential due to all external charges. The electrostatic interaction energy is then given by

$$\mathcal{H} = \int \rho(\vec{x})\phi(\vec{x})\,d^3x \tag{1}$$

where the integral is over the nuclear volume. $\phi(\vec{x})$ can be expanded in a power series about the nuclear center of mass, and such an expansion gives

$$\mathcal{H} = \int d^3x \rho(\vec{x}) \left\{ \phi_o + \sum_j \left(\frac{\partial \phi}{\partial x_j}\right)_o x_j + \frac{1}{2} \sum_{jk} \left(\frac{\partial^2 \phi}{\partial x_j \partial x_k}\right)_o x_j x_k + \cdots \right\}, \tag{2}$$

where the summation over each subscript extends from one to three and the subscript o indicates an evaluation at x equal to zero. It follows that

$$\mathcal{H} = Ze\phi_o + \sum_j P_j \left(\frac{\partial \phi}{\partial x_j}\right)_o + \frac{1}{2} \sum_{jk} Q'_{jk} \left(\frac{\partial^2 \phi}{\partial x_j \partial x_k}\right)_o + \cdots \tag{3}$$

where

$$\int d^3x \rho(\vec{x}) = Ze \quad = \text{nuclear charge} \tag{4}$$

$$\int d^3x \rho(\vec{x}) x_j = P_j \quad = \text{electric dipole moment} \tag{5}$$

$$\int d^3x \rho(\vec{x}) x_j x_k = Q'_{jk} \quad = \text{electric quadrupole moment} \tag{6}$$

The first term of Eq. (3) does not depend on the orientation of the nucleus and therefore is of no interest in magnetic resonance. The second term vanishes due to the inversion symmetry of the charge distribution. The third or quadrupole term, however, can affect the magnetic dipole transitions. The expression for $\mathcal{H}$ now becomes

$$\mathcal{H} = \frac{1}{2}\sum_{jk} Q'_{jk}\phi_{jk} , \quad \text{where } \phi_{jk} = \left(\frac{\partial^2 \phi}{\partial x_j \partial x_k}\right)_0, \tag{7}$$

and higher order terms in the expansion have been neglected. ϕ_{jk} is called the gradient of the electric field. ϕ_{jk} and Q'_{jk} are symmetric second rank tensors. It is possible to make Q'_{jk} traceless as well as symmetric by defining a new tensor as

$$Q_{jk} = 3Q'_{jk} - \delta_{jk}\sum_e Q'_{ee}, \tag{8}$$

where $\delta_{jk} = 1$ for $j=k$ and zero otherwise. The Hamiltonian then becomes

$$\mathcal{H} = \frac{1}{6}\sum_{jk} Q_{jk}\phi_{jk} - \frac{1}{6}\left(\sum_e Q'_{ee}\right)\left(\sum_j \phi_{jj}\right) . \tag{9}$$

The last term involves only traces and can be neglected.

The five components of Q'_{jk} can be related to one component. The charges in the nucleus are considered to precess very rapidly about the spin direction so that the external charges interact only with the time average of the nuclear charge distribution. Hence by symmetry $Q_{jk} = 0$ for

$j \neq k$ and $Q_{11} = Q_{22}$. But $Q_{11} + Q_{22} + Q_{33} = 0$, so that $Q_{11} = Q_{22} = -\frac{1}{2} Q_{33}$.

Ramsey (12) shows that the corresponding matrix elements of functions of the nuclear space coordinates like the electric quadrupole moment are proportional to the matrix elements of the angular momentum through a factor independent of m, which is the magnetic quantum number. Hence one can write that

$$\langle Im' | Q_{jk} | Im \rangle = C \langle Im' | \frac{3}{2}(I_j I_k + I_k I_j) - \delta_{jk} \vec{I}^2 | Im \rangle, \quad (10)$$

where $\vec{I}$ is the angular momentum of the nucleus in units of $h/2\pi$ and m assumes the values $-I, -I+1, \cdots I$.

The electric quadrupole moment, Q, is defined as the expectation value, in units of the electronic charge e, of Q_{33} in the state in which the component of I along the axis of symmetry is a maximum. Accordingly Q is of the form

$$eQ = \langle II | Q_{33} | II \rangle \quad \text{or} \quad eQ = \int \rho_{II}(\vec{x})(3z^2 - r^2) d^3x \quad (11)$$

where $\rho_{II}(x)$ is the expectation value of the nuclear charge density in the state where $m = I$. Then using Eq. (10) in Eq. (11), one obtains

$$eQ = C \langle II | 3I_z^2 - I^2 | II \rangle = C \left[3I^2 - I(I+1) \right], \quad (12)$$

or

$$C = \frac{eQ}{I(2I-1)} . \quad (13)$$

If one now combines Eq. (9), (10), and (13) and also writes $\mathcal{H}_Q$ for that part of the quadrupole interaction Hamiltonian of interest one obtains

$$\langle Im'|\mathcal{H}_Q|Im\rangle = \frac{eQ}{6I(2I-1)} \sum_{jk} \langle Im'|\tfrac{3}{2}(I_jI_k+I_kI_j)-\delta_{jk}\vec{I}^2|Im\rangle \phi_{jk}. \quad (14)$$

The electric quadrupole moment describes the departure from spherical symmetry of the nuclear charge distribution. Nuclei which have $I = 0$ or $I = 1/2$ can exhibit no electric quadrupole moment. The former exhibits no preferred orientation. The latter implies only a reversal of the spin direction and hence corresponds to the same effective charge distribution. The beryllium nucleus is known to have an angular momentum of $3/2\,\hbar$ so its charge distribution is not spherically symmetric (13).

The matrix elements of Eq. (14) can be obtained by using the matrix elements of the spin components $I_\pm = I_x \pm iI_y$. The only non-vanishing matrix elements of $\vec{I}$ are

$$\langle m|I_z|m\rangle = m$$

and

$$\langle m\pm1|I_\pm|m\rangle = \left[(I \mp m)(I \pm m + 1)\right]^{\frac{1}{2}}. \quad (15)$$

The quadrupole Hamiltonian can now be expressed in terms of the I_z, I_+ and I_-, giving

$$\langle m'|\mathcal{H}_Q|m\rangle = A\langle m'|(3I_z^2 - \vec{I}^2)\phi_{zz} + (I_+I_z + I_zI_+)\phi_{-1} + (I_-I_z + I_zI_-)\phi_1 + I_+^2\phi_{-2} + I_-^2\phi_2|m\rangle. \quad (16)$$

where

$$A = \frac{eQ}{4I(2I-1)},$$

$\phi_{\pm1} = \phi_{xz} \pm i\phi_{yz}$, and $\phi_{\pm2} = \frac{1}{2}(\phi_{xx} - \phi_{yy}) \pm i\phi_{xy}$.

Equation (16) can now be used to obtain all the matrix

elements of the quadrupole Hamiltonian which are needed to calculate the perturbations on the magnetic energy levels. These are

$$\begin{aligned}
\langle m|\mathcal{H}_Q|m\rangle &= A\left[3m^2 - I(I+1)\right]\phi_{zz} \\
\langle m \pm 1|\mathcal{H}_Q|m\rangle &= A(2m \pm 1)\left[(I \mp m)(I \pm m + 1)\right]^{\frac{1}{2}}\phi_{\mp 1} \qquad (17) \\
\langle m \pm 2|\mathcal{H}_Q|m\rangle &= A\left[(I \mp m)(I \mp m - 1)(I \pm m + 1)(I \pm m + 2)\right]^{\frac{1}{2}}\phi_{\mp 2} \\
\langle m'|\mathcal{H}_Q|m\rangle &= 0 \quad \text{for} \quad |m' - m| > 2 \ .
\end{aligned}$$

In the case that the quadrupole coupling energy is small compared to the magnetic level spacing one is able to treat $\mathcal{H}_Q$ as a perturbation on the magnetic energy $\mathcal{H}_M = -g\mu_o \vec{I}\cdot\vec{H}_o$, where $g = \mu/I\mu_o$ and $\mu_o = eh/2Mc$; hence

$$\mathcal{H} = \mathcal{H}_M + \mathcal{H}_Q$$

with energy levels given by

$$E_m = \sum_{k\geq 0} E_m^{(k)},$$

where $E_m^{(k)}$ is the k^{th} order perturbation on the magnetic levels

$$E_m^{(0)} = -m\mu H_o/I = -h\nu_L m \ , \ m = -I, -I+1, \cdots I. \qquad (18)$$

For an $I = 3/2$ there are four equispaced levels with an energy difference between levels equal to $2\mu H_o/3$. Hence the unperturbed resonance line actually consists of three superposed lines at the Larmor frequency $\nu_L = 2\mu H_o/3h$ with relative intensities 3:4:3.

The first order calculation yields

$$E_m^{(1)} = \frac{eQ}{4I(2I-1)}\left[3m^2 - I(I+1)\right]\phi_{zz}. \qquad (19)$$

The frequencies can be obtained from $h\nu_m = E_{m-1} - E_m$ which gives in first order

$$\nu_m^{(1)} = \frac{3eQ}{4I(2I-1)h}(2m - 1)\phi_{zz}. \qquad (20)$$

Here ϕ_{zz} is the second derivative of the electrostatic potential at the nuclear site, the z direction coinciding with the direction of the constant magnetic field. If one now makes the following substitutions:

$$E = 2\mu H_o/3 \;, \nu_L = E/h \;, \; K = \frac{3eQ(2m-1)}{2I(2I-1)h} \;, \text{ and } I = 3/2, \qquad (21)$$

one obtains for the energies and the frequencies to first order

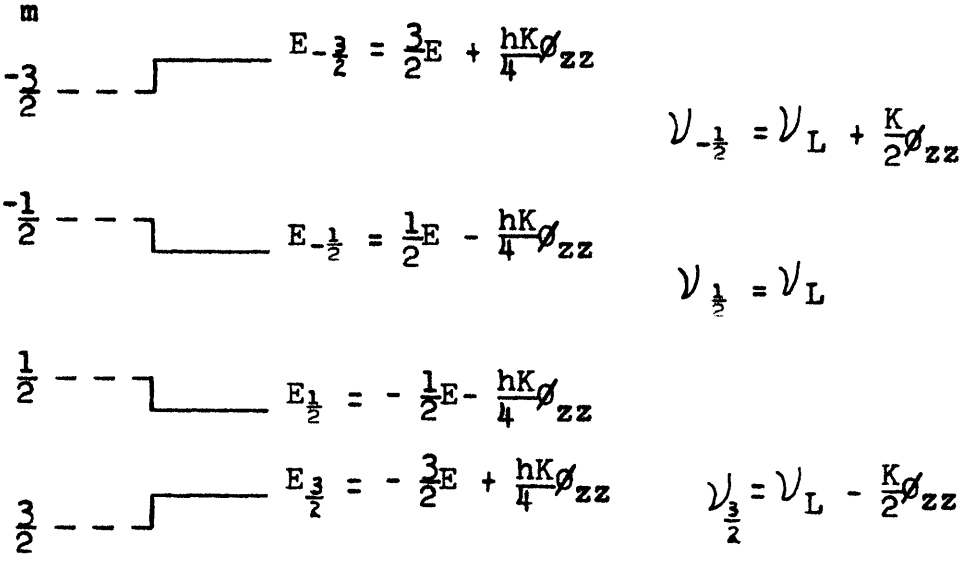

The dotted lines represent the magnetic levels and the solid lines represent the same levels perturbed by the quadrupole interaction in first order. One notes that in first order there remains a line at the Larmor frequency ν_L and

that the other two lines are symmetrically placed on either side of this central one; hence the name satellites for the shifted components. Also one observes that the frequency depends upon the value of ϕ_{zz} at the nuclear site so that there should be two satellites for each different site. The frequency difference is then given by

$$2\Delta\nu = K\phi_o = K\phi_{z'z'} \qquad (22)$$

where primes have been added to designate the direction of the constant magnetic field so that the unprimed symbols can later be used for the principal axes.

The perturbation to second order does shift the central component (4,p.336) and the outer lines are no longer symmetrically placed on either side. In the case of the beryllium sites there was no observable shift in the frequency of the central component.

B. Volkoff Method of Rotation Analysis

Volkoff and co-workers (17) begin by writing Eq. (22) as

$$2\Delta\nu = K\phi_{z'z'} = \frac{3(2m-1)}{2I(2I-1)} \cdot \frac{e^2qQ}{h} \cdot \frac{\phi_{z'z'}}{eq}, \qquad (23)$$

where the absolute value of e^2qQ/h is defined as the quadrupole coupling constant and eq is defined as the particular value of ϕ_{zz} that gives the largest value for the satellite separation.

The tensor ϕ_{jk} describes the magnitude of the electric field gradient at the nuclear site. It is symmetric by definition and also traceless, since $\nabla^2\phi = 0$. It is possible to assign a set of orthogonal axes XYZ fixed with reference to the crystal in terms of which ϕ_{jk} can be written as

$$\begin{pmatrix} \phi_{XX} & \phi_{XY} & \phi_{ZX} \\ \phi_{XY} & \phi_{YY} & \phi_{YZ} \\ \phi_{ZX} & \phi_{YZ} & \phi_{ZZ} \end{pmatrix} \qquad (24)$$

The XYZ axes in the chrysoberyl crystal will later be allowed to coincide with the crystallographic axes abc. It is possible to reduce this tensor with five independent components to a diagonal tensor with two independent components. To do so requires choosing a new set of xyz axes, called the principal axes. Then only ϕ_{xx}, ϕ_{yy}, and ϕ_{zz} remain and they are related by $\phi_{xx} + \phi_{yy} + \phi_{zz} = 0$.

If now one orders the ϕ's such that

$$\left|\phi_{zz}\right| \geq \left|\phi_{yy}\right| \geq \left|\phi_{xx}\right| \tag{25}$$

and also defines η, the asymmetry parameter, as

$$\eta = \frac{\phi_{xx} - \phi_{yy}}{\phi_{zz}} \tag{26}$$

then the new diagonalized tensor can be written

$$\begin{pmatrix} -eq(1-\eta)/2 & 0 & 0 \\ 0 & -eq(1+\eta)/2 & 0 \\ 0 & 0 & eq \end{pmatrix}. \tag{27}$$

The values of eq, η, and the direction cosines specifying the orientation of the xyz system with reference to the XYZ system would define the tensor. If the field gradient is axially symmetric, η, from Eq. (26), would be equal to zero. Should the field gradient have cubic symmetry or be spherically symmetric then $\phi_{xx} = \phi_{yy} = \phi_{zz}$, so that $\nabla^2\phi = 0$ would force each component to be equal to zero and the quadrupole interaction would disappear.

Let the x'y'z' axes refer to the laboratory system aligned so that z' will always be kept parallel to the direction of the constant magnetic field H_o. Let the X axis be set and held perpendicular to z' and parallel to y'. One can choose Y initially parallel to z' and with Z initially parallel to x'. Let the angle of rotation θ_X be measured between the Y and z' axis where $\theta_X = 0$ corresponds

to Y and z' being parallel. The transformation equations between the XYZ axes and the x'y'z' axes for the X rotation become

$$X = y' ,$$
$$Y = \cos\theta_X z' + \sin\theta_X x' , \qquad (28)$$

and $$Z = -\sin\theta_X z' + \cos\theta_X x' .$$

After several partial differentiations these give

$$\phi_{zz} = (\cos\theta_X \frac{\partial}{\partial y} - \sin\theta_X \frac{\partial}{\partial z})^2 \phi$$
$$= \frac{1}{2}(\phi_{YY} + \phi_{ZZ}) + \frac{1}{2}(\phi_{YY} - \phi_{ZZ})\cos 2\theta_X - \phi_{YZ}\sin 2\theta_X \qquad (29)$$

If Eq. (29) is substituted into Eq. (23) it gives

$$(2\Delta\nu)_X = A_X + B_X\cos 2\theta_X + C_X\sin 2\theta_X$$

or $$= A_X + R\cos 2(\theta + \delta_X) , \qquad (30)$$

where

$$A_X = \frac{1}{2}K(\phi_{YY} + \phi_{ZZ}) = -\frac{1}{2}K\phi_{XX} , \quad B_X = \frac{1}{2}K(\phi_{YY} - \phi_{ZZ}) ,$$
$$C_X = -K\phi_{YZ} , \quad \text{and} \quad R = (B_X^2 + C_X^2)^{\frac{1}{2}} \qquad (31)$$

The equations for the Y and Z rotations are similar and can be obtained from these by cyclic permutation of the subscripts. Thus one obtains three equations of the form of Eq. (30) and a total of twelve equations similar to Eq. (31). These equations serve to determine the elements of the $K\phi_{jk}$ tensor. By utilizing the conditions on the trace and by adding and subtracting the equations in Eq. (31) it is

possible to obtain the following relations between the various constants:

$$A_X + A_Y + A_Z = 0 \qquad A_Y + B_Y = A_X - B_X = -2A_Z$$
$$A_X + B_X = A_Z - B_Z = -2A_Y \qquad A_Z + B_Z = A_Y - B_Y = -2A_X \tag{32}$$

These identities can be employed to set the relative signs of the three curves and also to determine an average value for the constants.

The characteristic equation for the $K\phi_{jk}$ tensor can be expressed as

$$\gamma^3 - a\gamma - b = 0 \tag{33}$$

where $a = K^2(\phi_{XY}^2 + \phi_{YZ}^2 + \phi_{ZX}^2 - \phi_{XX}\phi_{YY} - \phi_{YY}\phi_{ZZ} - \phi_{ZZ}\phi_{XX})$,

$b = K^3(\phi_{XX}\phi_{YY}\phi_{ZZ} + 2\phi_{XY}\phi_{YZ}\phi_{ZX} - \phi_{XX}\phi_{YZ}^2 - \phi_{YY}\phi_{ZX}^2 - \phi_{ZZ}\phi_{XY}^2)$, (34)

and the b term is taken as positive. The solution of Eq. (33) is given by (15)

$$\gamma_n = 2(a/3)^{\frac{1}{2}}\cos(\alpha - 2\pi n/3) \quad n = 1,2,3 \tag{35}$$

where
$$\cos 3\alpha = (b/2)(3/a)^{\frac{3}{2}} \tag{36}$$

The characteristic roots are so ordered that γ_3 is positive and has the largest value, while γ_2 and γ_1 are both negative and γ_1 has the smallest absolute value. Their values are given by:

$$\gamma_1 = K\phi_{xx}\ ,\ \gamma_2 = K\phi_{yy}\ ,\ \text{and}\ \gamma_3 = K\phi_{zz}. \tag{37}$$

The asymmetry parameter is given by

$$\eta = \frac{\gamma_1 - \gamma_2}{\gamma_3} = \frac{\cos(\alpha - 2\pi/3) - \cos(\alpha - 4\pi/3)}{\cos(\alpha - 2\pi)} = \sqrt{3}\tan\alpha. \tag{38}$$

The quadrupole coupling constant can be found as follows

$$\left|\frac{e^2qQ}{h}\right| = \left|\frac{eQ\phi_{zz}}{h}\right| = \left|\frac{eQ}{hK}K\phi_{zz}\right| = \left|\frac{2I(2I-1)}{3(2m-1)}\gamma_3\right| , \qquad (39)$$

which for I = 3/2 gives

$$\left|\frac{e^2qQ}{h}\right| = \gamma_3 = K\phi_{zz} . \qquad (40)$$

Using any one of the three roots, say γ_1, and writing

$$\begin{aligned} (K\phi_{XX} - \gamma_1)w_x + K\phi_{XY}\, w_y + K\phi_{ZX}\, w_z &= 0 \\ K\phi_{XY}\, w_x + (K\phi_{YY} - \gamma_1)w_y + K\phi_{YZ}\, w_z &= 0 \\ K\phi_{ZX}\, w_x + K\phi_{YZ}\, w_y + (K\phi_{ZZ} - \gamma_1)w_z &= 0 \end{aligned} \qquad (41)$$

where the w's are the characteristic vectors associated with γ_1, one can at once solve any two of these for the direction cosines λ_1, μ_1, and ν_1. For example λ_1 would be given by

$$\lambda_1 = \frac{w_x}{(w_x^2 - w_y^2 - w_z^2)^{\frac{1}{2}}} . \qquad (42)$$

Repeating the above procedure for the other two roots would give all nine direction cosines. The relative signs for the three direction cosines obtained from each root would be fixed but the absolute sign for each set would not be determined. If these calculations are carried out it is possible to express all nine direction cosines in the following manner.

$$\frac{\lambda_n}{D_{1n}} = \frac{\mu_n}{D_{2n}} = \frac{\nu_n}{D_{3n}} = \frac{\pm 1}{(D_{1n}^2 + D_{2n}^2 + D_{3n}^2)^{\frac{1}{2}}} \quad n = 1,2,3 \qquad (43)$$

$$\text{with} \quad D_{1n} = K^2\phi_{XY}\phi_{YZ} - K\phi_{ZX}(K\phi_{YY} - \gamma_n)$$
$$D_{2n} = K^2\phi_{ZX}\phi_{XY} - K\phi_{YZ}(K\phi_{XX} - \gamma_n) \qquad (44)$$
$$D_{3n} = (K\phi_{XX} - \gamma_n)(K\phi_{YY} - \gamma_n) - K^2\phi_{XY}^2$$

It is sometimes possible to learn from crystal symmetry that a particular one of the XYZ axes is parallel to a principal axis. If one assumes that the Z axis coincides with one of the principal axes then one would know that $\phi_{YZ} = \phi_{ZX} = 0$ and that $C_X = C_Y = 0$. The tensor would then be of the form

$$\begin{pmatrix} K\phi_{XX} & K\phi_{XY} & 0 \\ K\phi_{XY} & K\phi_{YY} & 0 \\ 0 & 0 & K\phi_{ZZ} \end{pmatrix} \quad \text{or} \quad \begin{pmatrix} (A_Z + B_Z) & -C_Z & 0 \\ -C_Z & (A_Z - B_Z) & 0 \\ 0 & 0 & -2A_Z \end{pmatrix} \qquad (45)$$

where the constants are obtained from the equation for the Z rotation, that is

$$(2\Delta\nu)_Z = A_Z + B_Z\cos 2\theta_Z + C_Z\sin 2\theta_Z. \qquad (46)$$

The characteristic roots would be given by

$$\gamma_1 = -2A_Z \quad \text{and} \quad \gamma_{2,3} = A_Z \pm (B_Z^2 + C_Z^2)^{\frac{1}{2}}. \qquad (47)$$

The principal axes corresponding to $-2A_Z$ would be parallel to the Z axis and the direction cosines with respect to the X axis for the other two principal axes would be obtained from

$$\lambda_n = \frac{C_Z}{\left[C_Z^2 + (\gamma_n - A_Z - B_Z)^2\right]^{\frac{1}{2}}} \quad n = 2,3 \qquad (48)$$

The above analysis allows one to determine the quadrupole coupling constant, the asymmetry parameter, and the orientation of the principal axes of the electric field gradient at the nuclear site.

C. Crystal Structure of Chrysoberyl

Chrysoberyl ($BeAl_2O_4$) exhibits an orthorhombic structure with the following values for its crystallographic axes (18)

$$a=4.42,\ b=9.39,\ \text{and}\ c=5.47A.$$

Its unit cell contains four molecules so that there are four atoms of beryllium and eight atoms of aluminum in each unit cell. The sixteen oxygen atoms in the unit cell are arranged in a nearly hexagonal close-packed array with the much smaller metallic ions in interstitial positions. Bragg and Brown (3) have performed an X-ray study of chrysoberyl in which they find that each aluminum atom occupies a space between six of the oxygen atoms. They also find that there are two types of sites for the aluminum atom with half of the aluminum atoms at symmetry centers and half of them on reflection planes. This fact is also verified by the work of Hockenberry, Brown, and Williams (8) in their nuclear resonance studies of aluminum in chrysoberyl. They find that there are two types of aluminum sites and that one of the sites does have a principal axis perpendicular to the reflection planes.

The beryllium atoms cannot be located by X-ray diffraction analysis since the atoms are so light that their positions cannot be established in this manner. The positions of the beryllium atoms in chrysoberyl are assigned as the same positions that the silicon atoms occupy in olivine

(Mg_2SiO_4). Figures I and II illustrate the beryllium atoms in the positions occupied by the silicon atoms in olivine. This assignment places each of the beryllium atoms at the center of a tetrahedron consisting of four oxygen atoms at the corners of the tetrahedron. This assignment also places two of the beryllium atoms on one of the reflection planes and the other two atoms of beryllium on the other reflection plane.

Figure I illustrates the unit cell of chrysoberyl projected on its a-plane. The large, medium, and small circles are used to represent the oxygen, aluminum, and beryllium atoms respectively. The numbers written within each circle represent the approximate fractional height above the a-plane in units of the crystallographic length a. Note that a circle with a zero would represent two atoms, one above the other, a distance a apart.

Figure II is a photograph of a model of chrysoberyl where the dark spheres represent beryllium atoms, the large light spheres represent oxygen atoms, and the small light spheres represent aluminum atoms.

In the a-plane projection the four beryllium atoms are at different heights as specified by the fractions 1/8, 3/8, 5/8, and 7/8. These fractions can be employed to designate the individual beryllium atoms. Thus one can state that the 3/8 atom and the 1/8 atom are on the same reflection plane.

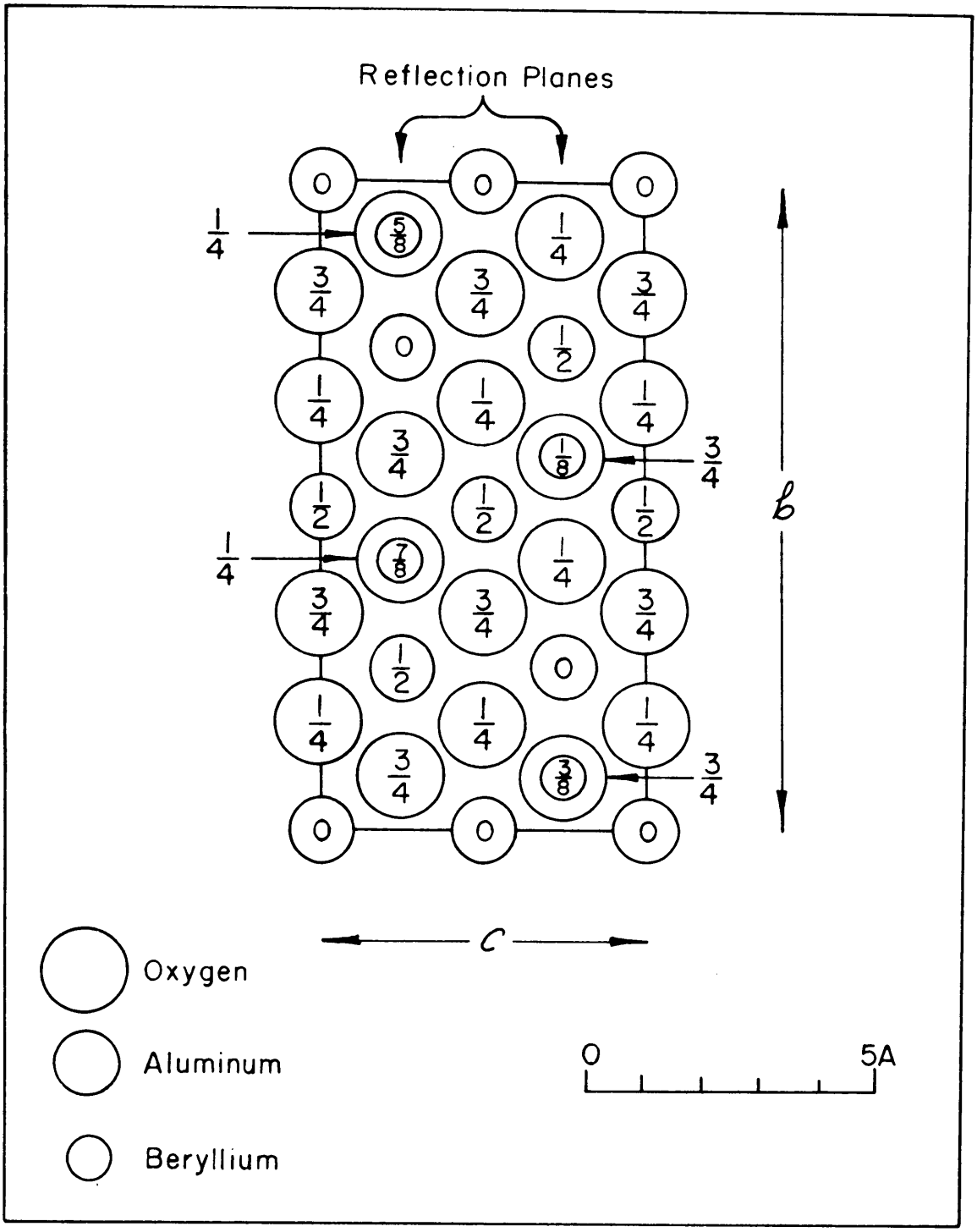

FIGURE I — UNIT CELL OF CHRYSOBERYL ($BeAl_2O_4$)

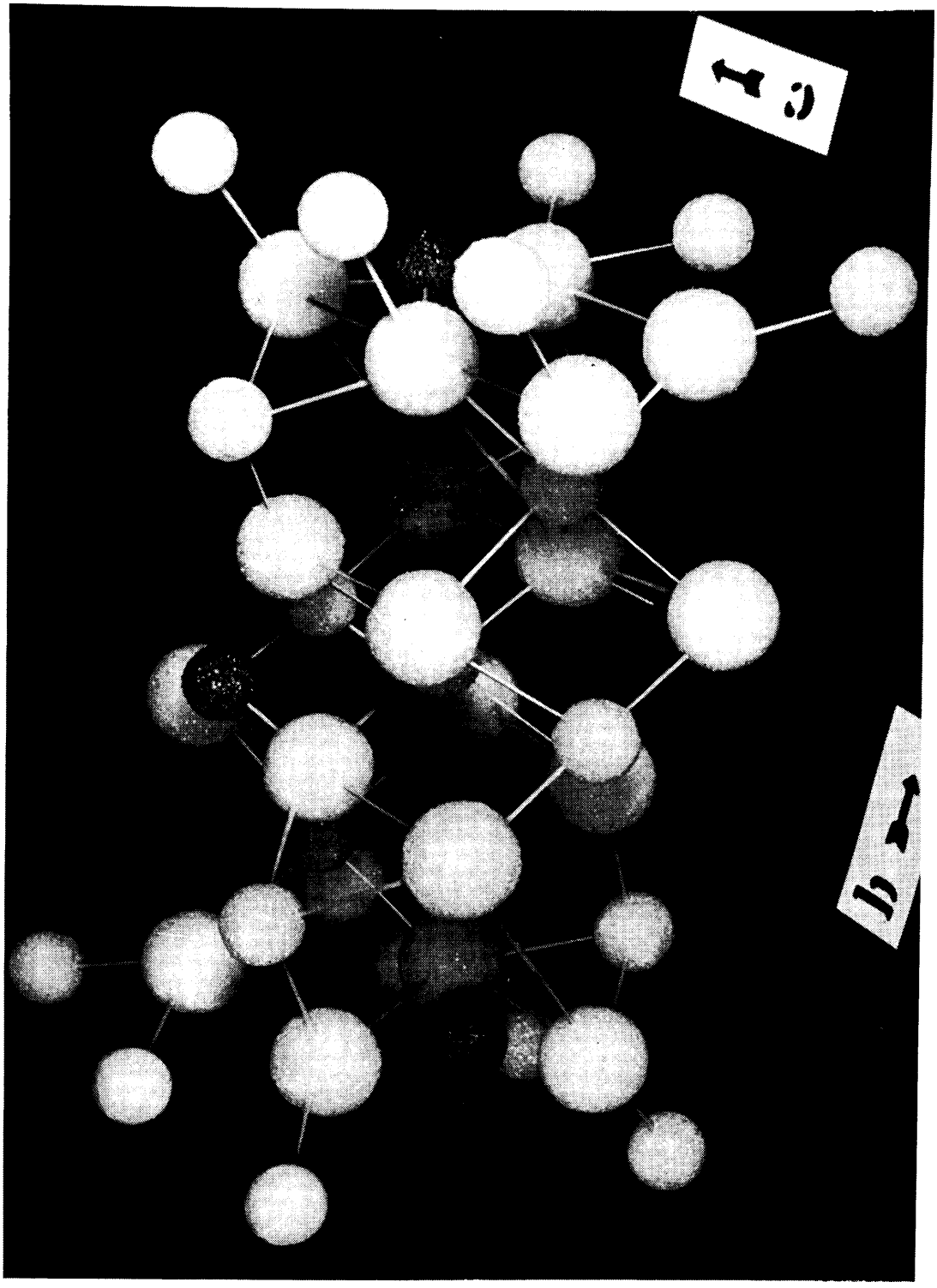

FIGURE II. PHOTOGRAPH OF A CHRYSOBERYL MODEL

These reflection planes are parallel to one another and parallel to the ab plane, hence one of the principal axes of the field gradient is perpendicular to the ab plane and parallel to the c axis.

The environment of the 1/8 atom can be made identical to the 7/8 atom by a 180 degree rotation about an axis through the 1/8 atom and parallel to the c axis. Since only the directions of the field gradient are determined and not their senses these two sites would exhibit the same field gradient. Two such sites are called identical sites. The same argument can be used to show that the site of the 3/8 atom and the site of the 5/8 atom are also identical.

A mirror parallel to the bc plane and passing through the oxygen atoms of height 3/4 would reflect the environment of the 7/8 atom into the same environment as the 5/8 atom. If the principal axes were all parallel to the crystallographic axes this reflection would give identical sites at the 7/8 atom and at the 5/8 atom. If the principal axes were not parallel to the crystallographic axes this reflection would give the same values for the field gradient but a different orientation of the principal axes at the two sites. Two such sites that have the same principal components for their field gradient but differ in orientation are called equivalent sites.

There is at least another possible set of four sites for the beryllium atoms that would place two of them on one reflection plane and two on the other reflection plane. These sites would also surround each beryllium atom with four oxygen atoms. Two of these would be identical sites with respect to each other and the other two sites would also be identical with respect to each other. Using arguments similar to the ones used previously one determines that the components of the field gradient at the four sites could at most differ only in orientation so that these four sites would also be at least equivalent to each other. In fact the set of four sites first discussed and this set of four sites each consist of two pairs of sites, the sites in each pair are identical and the sites in different pairs are equivalent.

III. EXPERIMENTAL APPARATUS AND PROCEDURE

A. Nuclear Magnetic Resonance Spectrometer

The block diagram of the nuclear magnetic spectrometer is given in Figure III. The most important component of the spectrometer is the oscillating detector. It was designed by T. L. Collins (17) at the University of British Columbia and constructed by T. E. Gilmer, Jr. of the Virginia Polytechnic Institute Physics Department. The circuit diagram for the oscillating detector is given in Figure IV and a photograph of it appears in Figure V.

The crystal sample is placed inside the coil L in order to study its resonance spectra. The coil L is wound in the form of a solenoid with a diameter just large enough to allow the crystal to fit inside. The crystal and the coil are placed inside the small brass box at the end of the arms in Figure V and then the box is placed in the steady magnetic field. The coil L and the capacitors C_1, form the resonant circuit of the oscillating detector. The oscillations are maintained by two 6AG5 pentodes operating in push-pull. The feedback which controls the amplitude of the radio frequency oscillations is adjusted by varying the capacitors C_2.

The resonant circuit is coupled through a small capacitor to the control grid of a third 6AG 5 which gives one stage

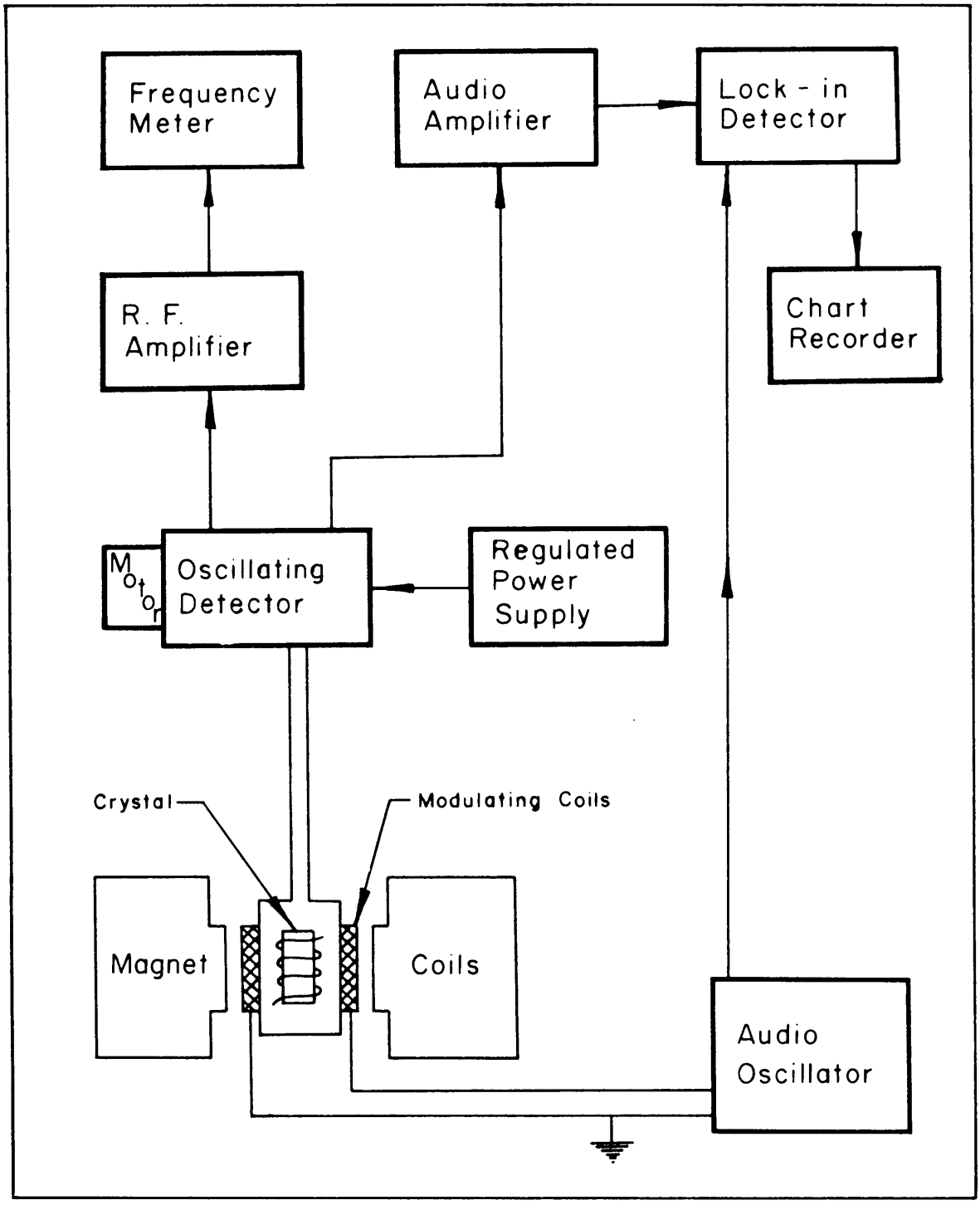

FIGURE III — BLOCK DIAGRAM OF THE SPECTROMETER

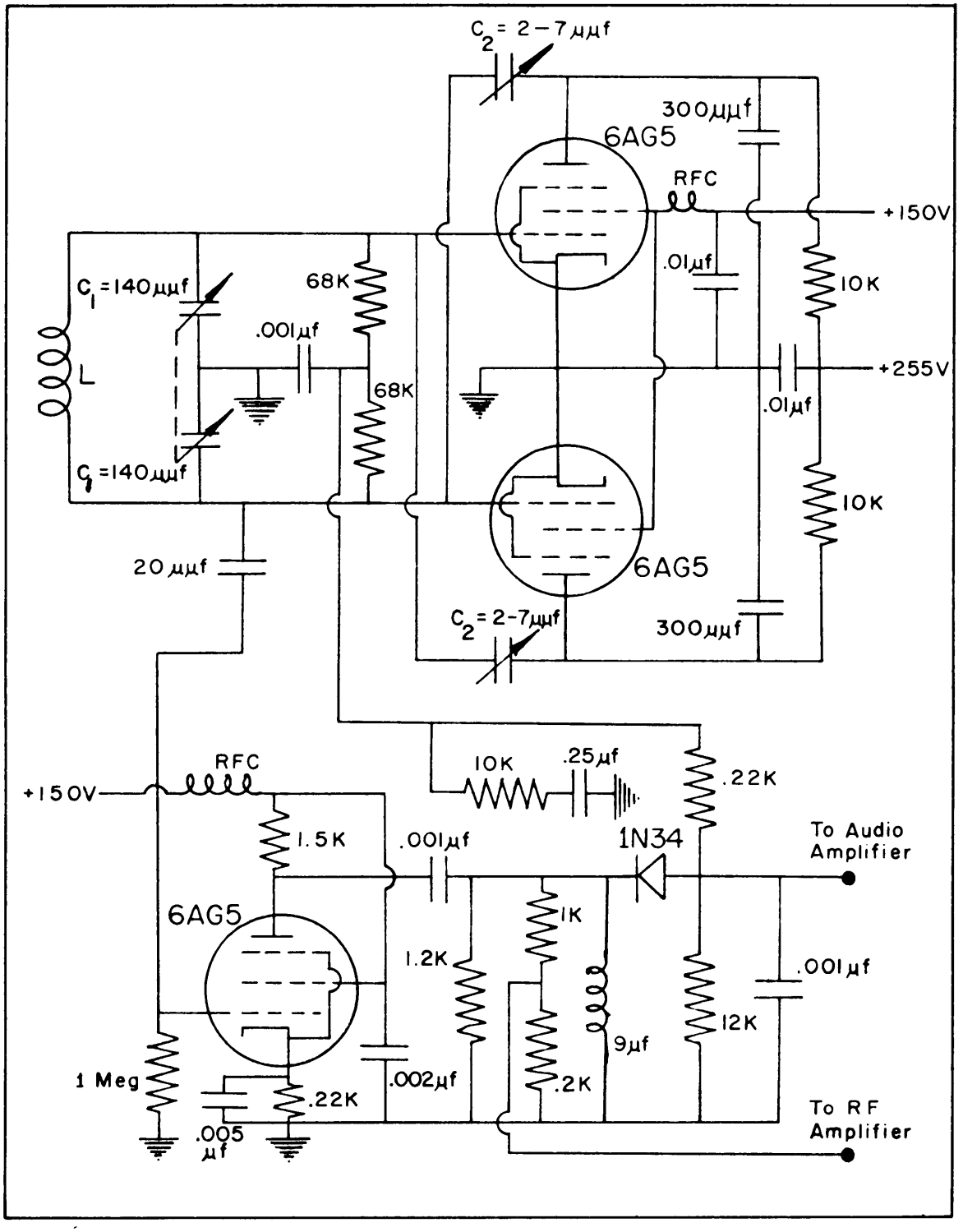

FIGURE IV - CIRCUIT DIAGRAM OF THE OSCILLATING DETECTOR

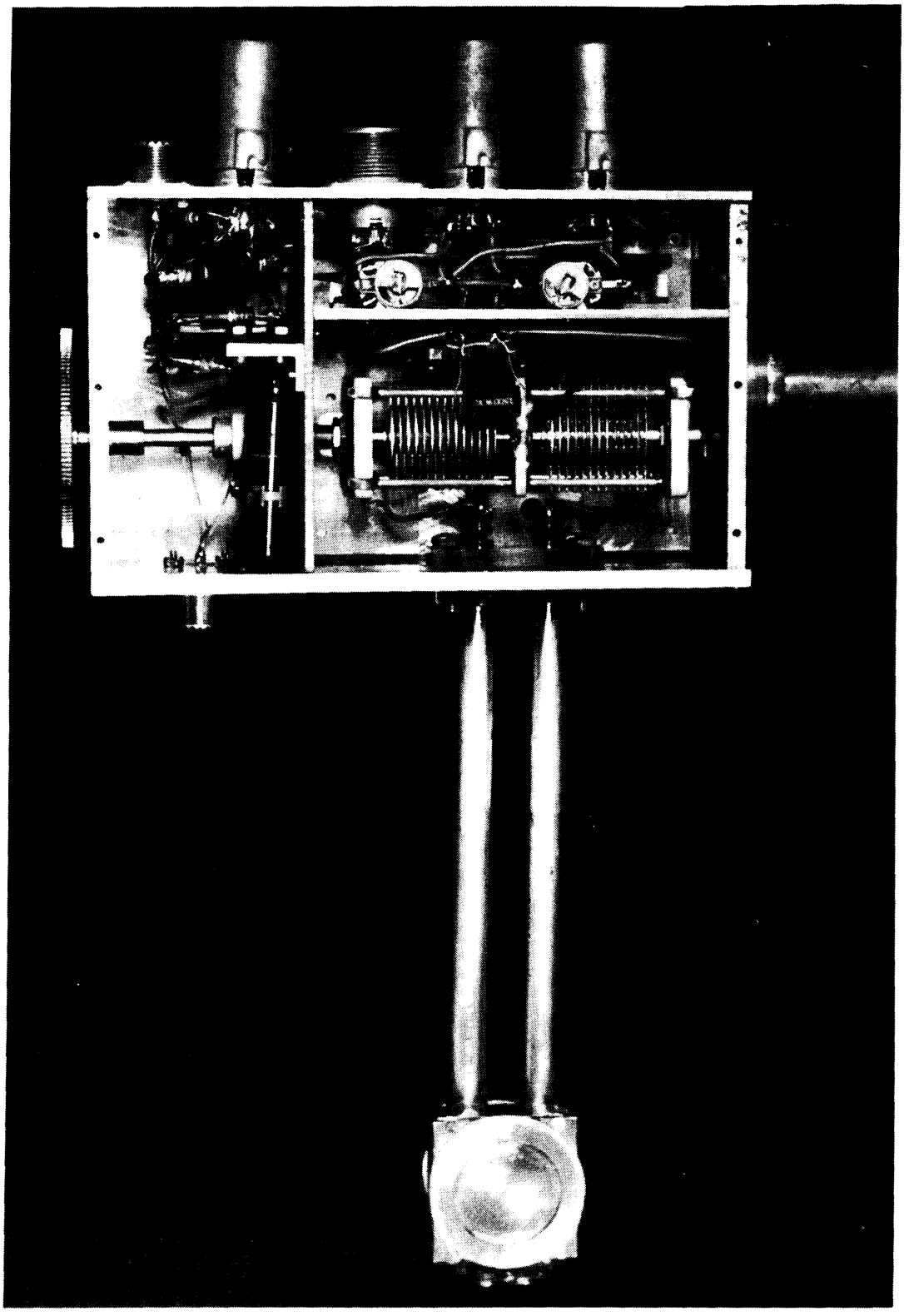

FIGURE V. PHOTOGRAPH OF THE OSCILLATING DETECTOR

of amplification before rectification. The rectification is performed by a 1N34 crystal diode. A fraction of this d.c. rectified signal is now fed back through an a.v.c. circuit to the control grids of the oscillator tubes in order to keep the oscillation level low. A regulated power supply is used to supply the power to the oscillating detector (5).

A quarter r.p.m. motor and four reduction gears are mounted on the top of the oscillating detector. These are connected by a shaft to the tuning capacitors so that the oscillation frequency is varied slowly. The rate of change in the frequency selected for the chrysoberyl sample is approximately six kilocycles per sec. per min. This rate gives a strong signal for the satellites and still allows the longest sweeps to be completed in less than an hour.

The steady magnetic field is provided by a Varian Associates Model V4012A Electromagnet which is rated to produce magnetic fields in excess of 13,000 gauss. This electromagnet has 12 inch diameter poles pieces with a gap width of 1.75 inches. The power supply for the electromagnet is the Varian Associates Model V2100B Regulated Magnet Power Supply. It is rated to supply a maximum current of two amperes with a power output of five kw. and to regulate the current to one part in 10,000 against a line voltage change of 10 percent (16). This system is capable of maintaining

very homogeneous fields. But with chrysoberyl high homogeneity is not required since the lines are broad (approximately 20 gauss) and to first order the splitting is independent of the magnetic field strength.

The steady magnetic field is modulated by applying a 315 cps. signal across two modulating coils on the outside of the sample box. This signal is derived from a Hewlett Packard Model 201C audio oscillator and gives a field modulation of approximately one gauss which is small compared to the width of the chrysoberyl resonances. If the radio frequency is varied slowly through a resonance, without the audio modulation applied, all one observes is an absorption curve indicated by a dip in the rf level in the tank circuit. But with the applied audio signal one observes a modulation of the rf level and the amplitude of this modulation varies as the slope of the absorption curve instead of as the absorption curve itself. The applied audio signal and the audio modulation of the radio frequency are in phase on that part of the absorption curve with a positive slope and out of phase on that part with a negative slope. The phase change occurs at the minimum of the absorption curve. Thus the signal on passing through resonance that leaves the oscillating detector is a rectified radio frequency carrier with an audio modulation which changes phase with respect to the audio signal applied to

the modulating coils.

The signal from the oscillating detector next goes to an R.C.A. Model WV73A Audio Voltmeter for audio amplification which also removes the radio frequency component from the signal. It then goes to the lock-in detector. The circuit diagram for the lock-in detector (17) is shown in Figure VI. The lock-in detector also receives another audio signal from the audio oscillator. The phase of this signal with respect to the signal from the oscillating detector is adjusted by the phase shifter which is a variable auto transformer in series with the line followed by a $4\mu f$ capacitor in parallel with the line. This adjustment allows the lock-in detector to supply a stable d.c. signal to the recorder while searching for a resonance. The lock-in detector supplies a signal that increases first in one direction, decreases in that direction and then increases and decreases in the opposite direction as a resonance is traversed. This recorded curve approximates the derivative of the absorption curve with respect to frequency.

The lock-in detector operates as follows: The one megohm resistor and one of the three large capacitors, usually the $8\mu f$ capacitor, integrate the difference of potential that appears across the previous elements for a large number of cycles. The diode network acts somewhat as a switch having a small resistance when it conducts in

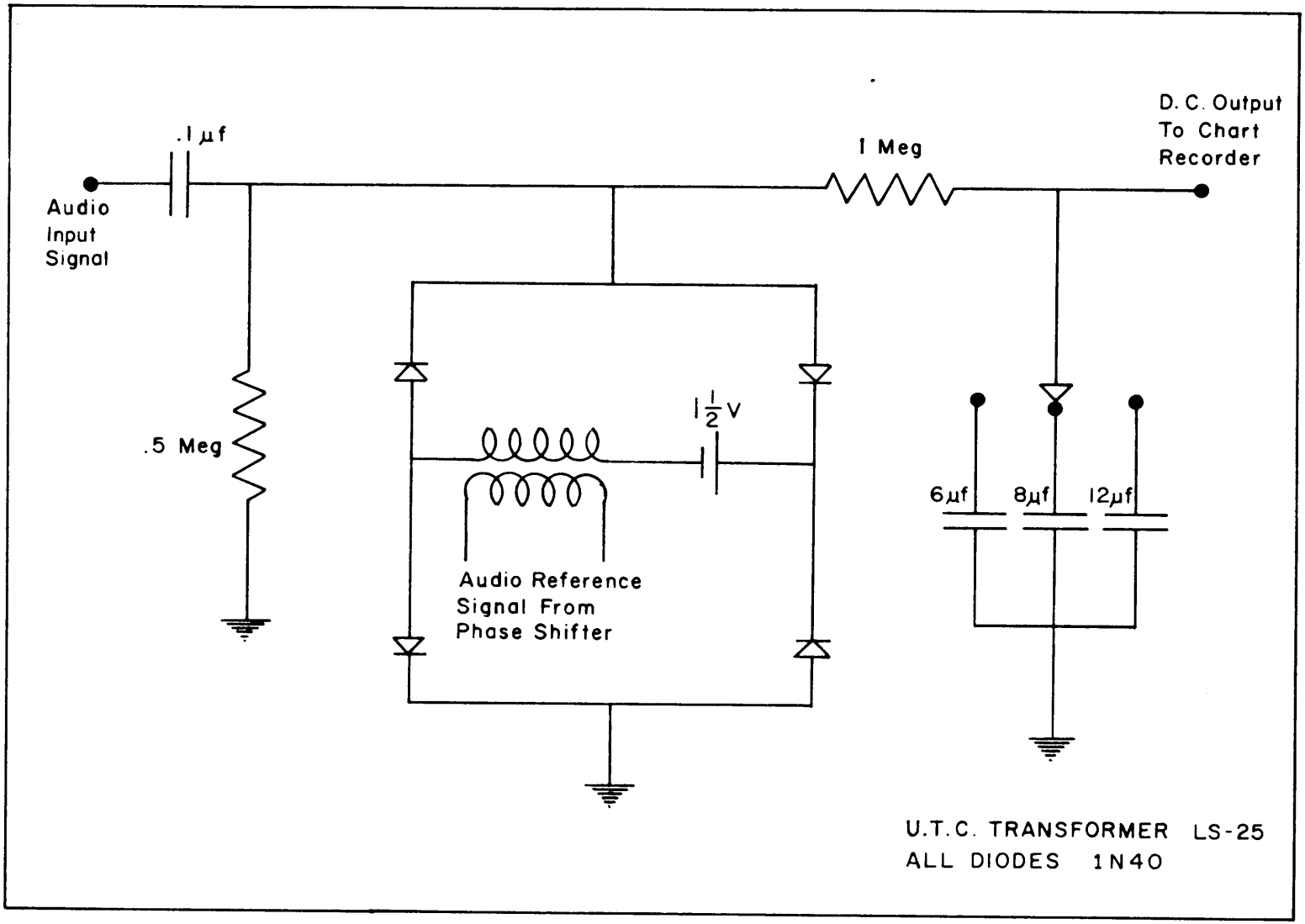

FIGURE VI - CIRCUIT DIAGRAM OF LOCK-IN DECTECTOR

either direction and a large resistance when it does not conduct. The reference signal is adjusted in phase and amplitude so that the "switch" is closed part of every cycle and so that the integrated voltage over many cycles is held constant. However during a resonance the amplitude and phase of the audio input signal change so that the switch is closed for differing lengths of time and over differing intervals of the cycle. This produces the varying d.c. output that is sent to the chart recorder. A Varian Associates Model G11A chart recorder is used to record the resonances. It has a 10 millivolt span and is usually operated at a chart speed of four minutes per inch.

A small rf signal is removed from the oscillating detector following the amplification stage and is fed to several Hewlett Packard Model 460A wide band amplifiers. From there it is sent to a Hewlett Packard Model 524C Frequency Meter to measure its frequency. The frequency is read and recorded on the moving chart at frequent time intervals.

B. Preparation of the Sample

The original chrysoberyl crystal had prominent striations on its [100] face. This allowed the directions of the orthorhombic axes to be determined by inspection (3). It was first cut with a diamond saw in such a manner as to obtain a sample that was roughly rectangular and with the striations approximately along the longest dimension of the rectangle. It was then ground until it was approximately cylindrical with a diameter of about one cm and a length of two and a half cm. This crystal was mounted on a straight aluminum rod with black wax. An optical collimator was used to align the striations vertically and hence the c axis would be parallel to the aluminum rod.

An aluminum block with a plastic sheet along one side was mounted between the pole pieces of the electromagnet with the plastic sheet against one pole piece for protection. Four brass set screws with plastic guards on their ends were set in the opposite side of the aluminum block. These four set screws were backed out of the aluminum block until they fit snugly against the opposite pole piece of the electromagnet, and thereby held the aluminum block in position. A hole was drilled through the aluminum block of nearly the same diameter as the aluminum rod that is fastened to the sample. This hole was drilled in the block so that it would be parallel to the pole pieces and if extended

downward would pass through the center of the magnetic field. A scale with one degree intervals marked on it was mounted above the aluminum block.

The aluminum rod, with the crystal attached to one end, was inserted in the lower end of the hole. The rod was drawn up until the crystal just touched the bottom of the aluminum block. The sample box on the end of the oscillating detector was inserted and centered in the magnetic field below the crystal. The crystal was then lowered into the rf coil contained in the sample box by lowering the aluminum rod.

A pointer was attached to the aluminum rod immediately above the scale. The pointer was set visually to read 90 deg when the plane containing the striations was set approximately parallel to the magnetic field. After all the resonance sweeps were completed on the sample the optical collimator was used to calibrate the angle settings referred to a line perpendicular to the plane containing the striations.

The original crystal was large enough so that two more samples of about the same dimensions as the first one could be obtained. Each of these crystals also contained prominent striations. They were prepared and mounted in a similar fashion to the one discussed above. The second crystal was mounted with the plane of the striations again

vertical but the striations this time being horizontal. The third crystal was mounted with the plane containing the striations on the bottom of the crystal and horizontal.

A rotation of the first sample as mounted would be a rotation about the c axis which will be designated as the Z rotation. The second would be a rotation about the b axis or the Y rotation. The third would be an a rotation or the X rotation.

C. Measurement Technique

The first quadrupole splitting obtained with this spectrometer was that of aluminum in ruby (Al_2O_3). This was an artificial single crystal with chromium impurities added and was grown to be used as a ruby laser. It gave the characteristic spectrum of five lines due to I = 5/2 for aluminum and also due to the fact that all of the aluminum atoms are in identical sites (10). A strong and broad resonance was observed in a single crystal of boron due to B^{11}. No satellites were ever observed probably due to the extremely complex crystal structure of this crystal which would indicate many different types of sites for the B^{11} nuclei (7).

A single crystal of sodium nitrate ($NaNO_3$) was grown and the quadrupole splitting of the Na^{23} nuclei was observed. This crystal gave the characteristic three lines due to I = 3/2 for sodium and identical sites for this nucleus in sodium nitrate (10). Also several of the aluminum lines and the second order shift in the aluminum central resonance were observed in chrysoberyl.

The resonance frequency for beryllium is 5.983 Mc in a field of 10^4 gauss. A 56 $\mu\mu$f capacitor was placed in parallel with the capacitors C_1 in order to lower the operating frequency range of the oscillating detector to the

region of six to eight Mc which corresponds to a magnetic field region of 1.003×10^4 to 1.337×10^4 gauss for Be^9. The central resonance for beryllium appeared at 7.141 Mc which corresponds to a magnetic field of 1.194×10^4 gauss. During all of the runs on all three of the samples this resonance frequency never varied by more than three kc from the above value. This included a period of almost a month and also included turning the magnet up and down many times during this period.

The c or Z rotation measurements were performed first and in the following manner: A particular position for the crystal was set on the angular scale. The frequency of the oscillating detector was lowered several hundred kc below the central resonance frequency by manually rotating the tuning capacitors. The frequency was then increased slowly by the drive motor connected to the tuning capacitors. The frequency was recorded on the edge of the chart at 13 kc intervals. The central resonance and the satellites were very nearly symmetric so that their centers were estimated visually on the chart. The frequencies corresponding to their centers were obtained by interpolation on the chart between the two recorded frequencies on either side of the center.

The crystal was rotated to a new position and the above procedure was repeated. Once the approximate position of the

lower satellite was known from a previous sweep the initial frequency for the following sweep could be manually set so that there would be little search time required before the lower satellite appeared. Also on the long sweeps, where the satellites were far from the central resonance, the central resonance could be omitted by manually increasing the frequency over the central portion of the spectrum but recording the satellites in the usual manner. This procedure shortened the length of time required for the long sweeps.

A sweep was performed at every five degree position of the crystal over a 180 deg interval and then at every ten deg position over the second 180 deg interval. This procedure was then repeated for the b and a rotations. Occasionally a particular sweep would be repeated both in angular sequence and out of sequence and also before and after the magnet had been shut down and then restored. The frequency interval between a pair of satellites measured on a repeat sweep and the frequency interval measured on the original sweep was always less than two kc.

Figure VII illustrates two typical chart recorder traces. These two traces were both taken from the c rotation group. The upper trace shows the two sets of satellites obtained on all c rotation traces. The lower trace shows the two sets of satellites coalesed so that they appear as just one large pair of satellites.

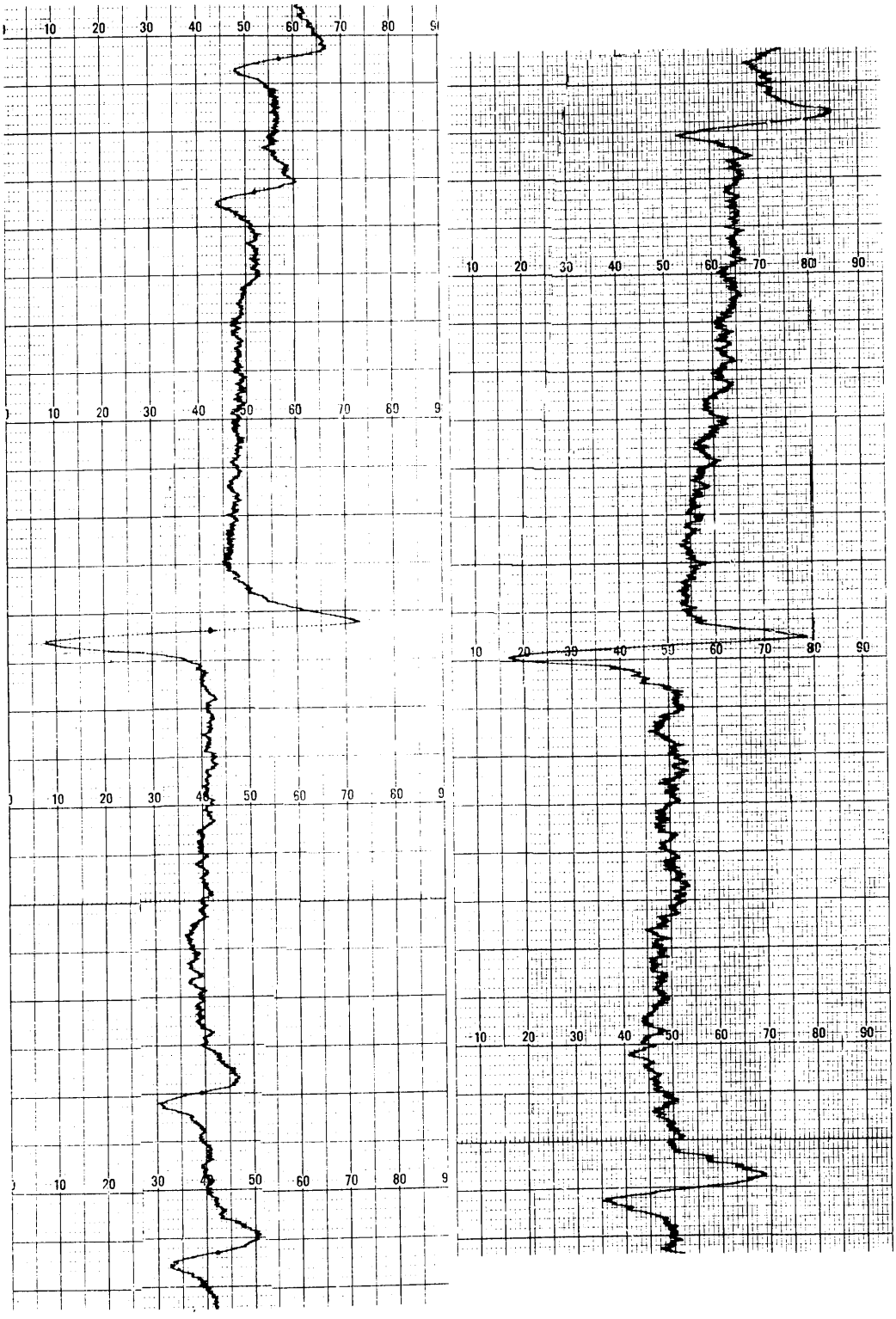

Figure XII Typical N.M.R. Recorder Traces

IV. RESULTS AND DISCUSSION

A. Analysis and Interpretation of Data

The frequency interval $2\Delta\nu$ between each pair of satellites is obtained directly from the recorder chart by subtracting the frequency of one satellite from the frequency of the other satellite in the pair for each position of the crystal. These frequency intervals are plotted versus the angle of rotation of the crystal as the experimental points in Figures VIII, IX, and X. Figure XI shows the three curves plotted together and to the same scale. The solid curve in each figure is obtained by a least squares fit (14) of the experimental points to Eq. (30) with the use of an I.B.M. 1620 computer. These curves are shown plotted zero to 180 deg but the experimental points over the entire 360 deg are used to obtain the solid curves. In each rotation there exist two separate positions of the crystal such that a crystallographic axis coincides with the direction of the steady magnetic field. These positions are indicated on the curves by a, b, and c. Thus a on one of the graphs, for example, is used to indicate that the a axis coincides with the direction of H_o at this position.

The equations for the curves are as follows: For the X or a rotation in Figure VIII one obtains

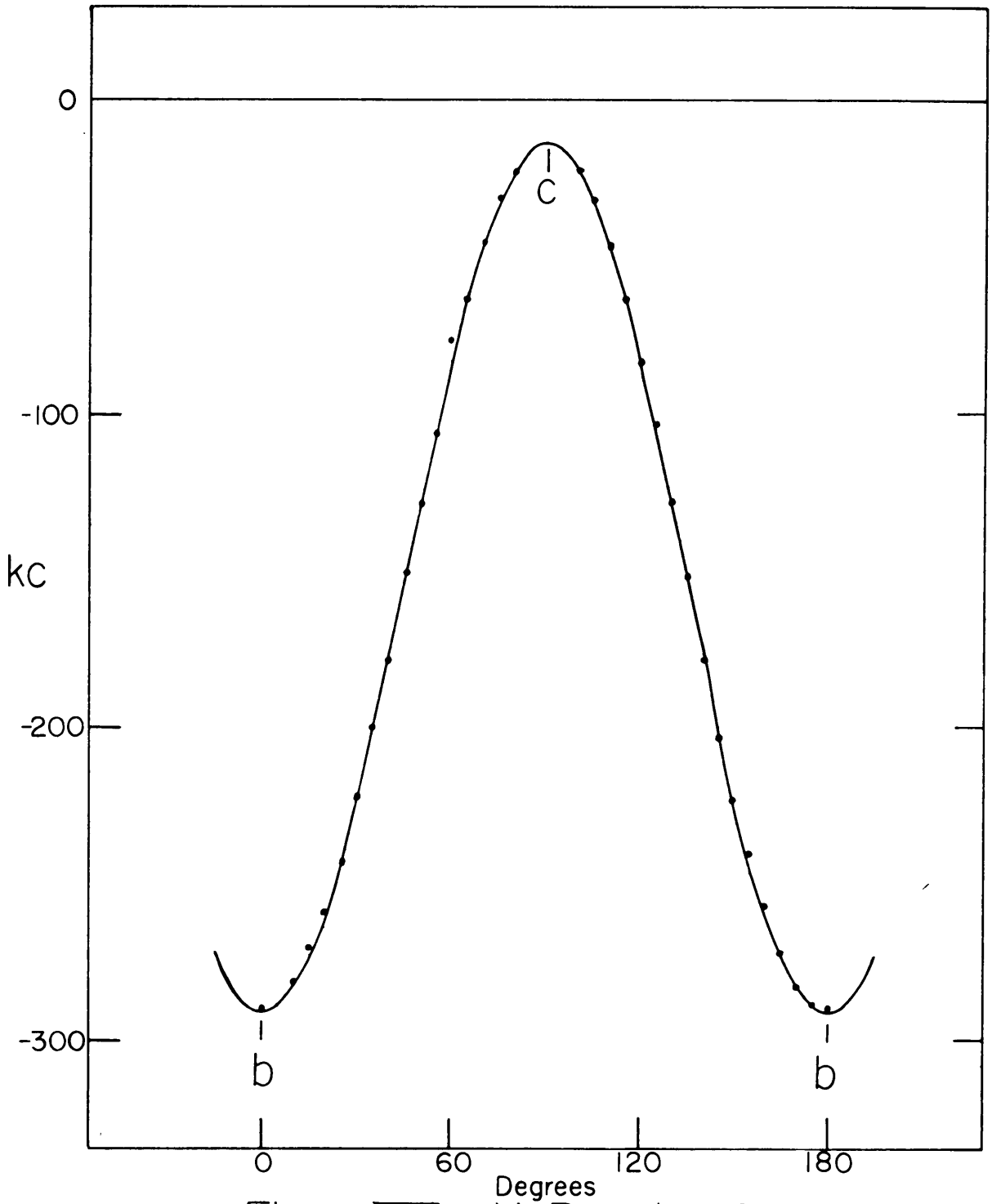

Figure VIII X Rotation Graph

Frequency Interval Between Satellites Versus the Angle Between the Y Axis and H_o

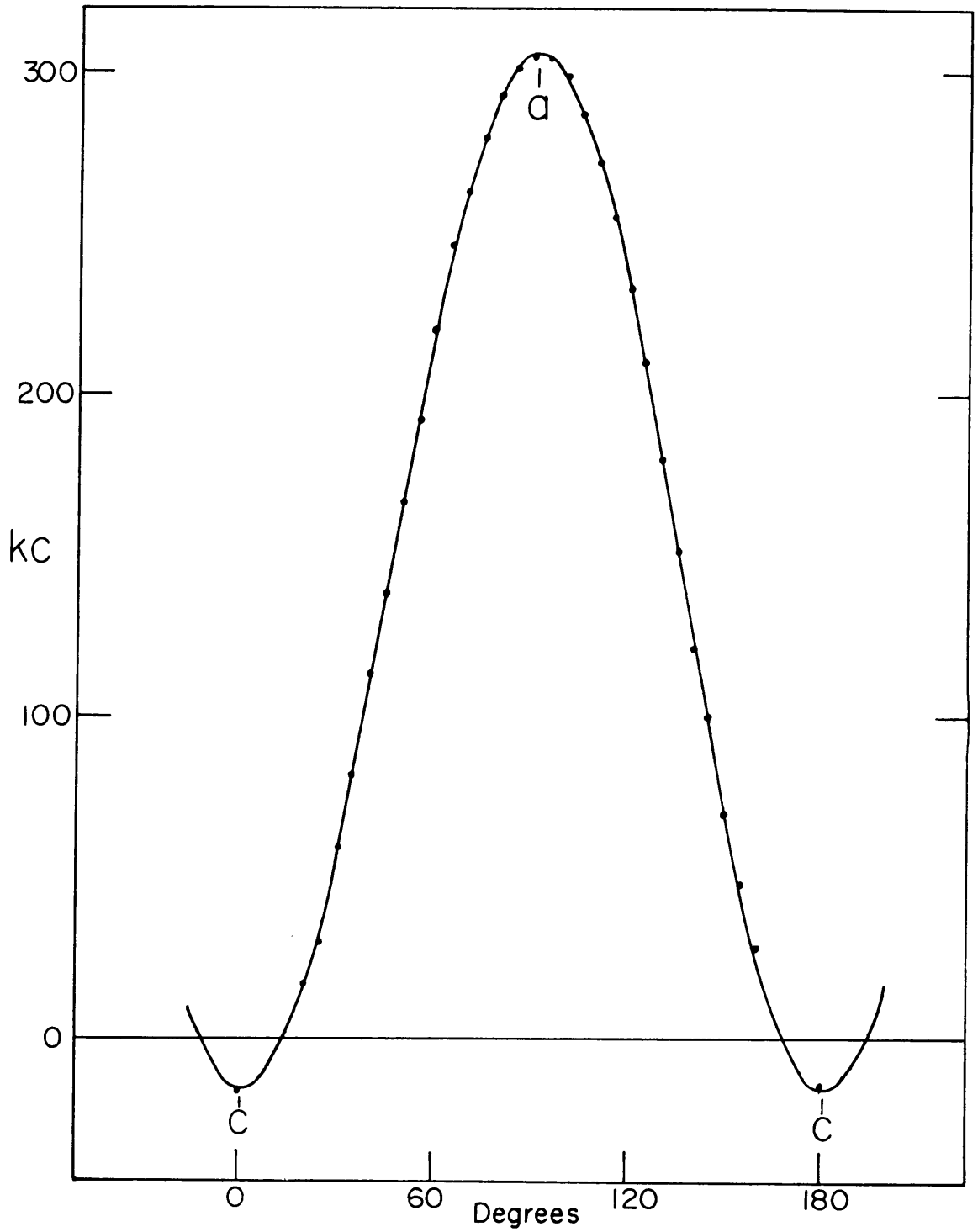

Figure IX Y Rotation Graph

Frequency Interval Between Satellites Versus the Angle Between the Z Axis and H_o

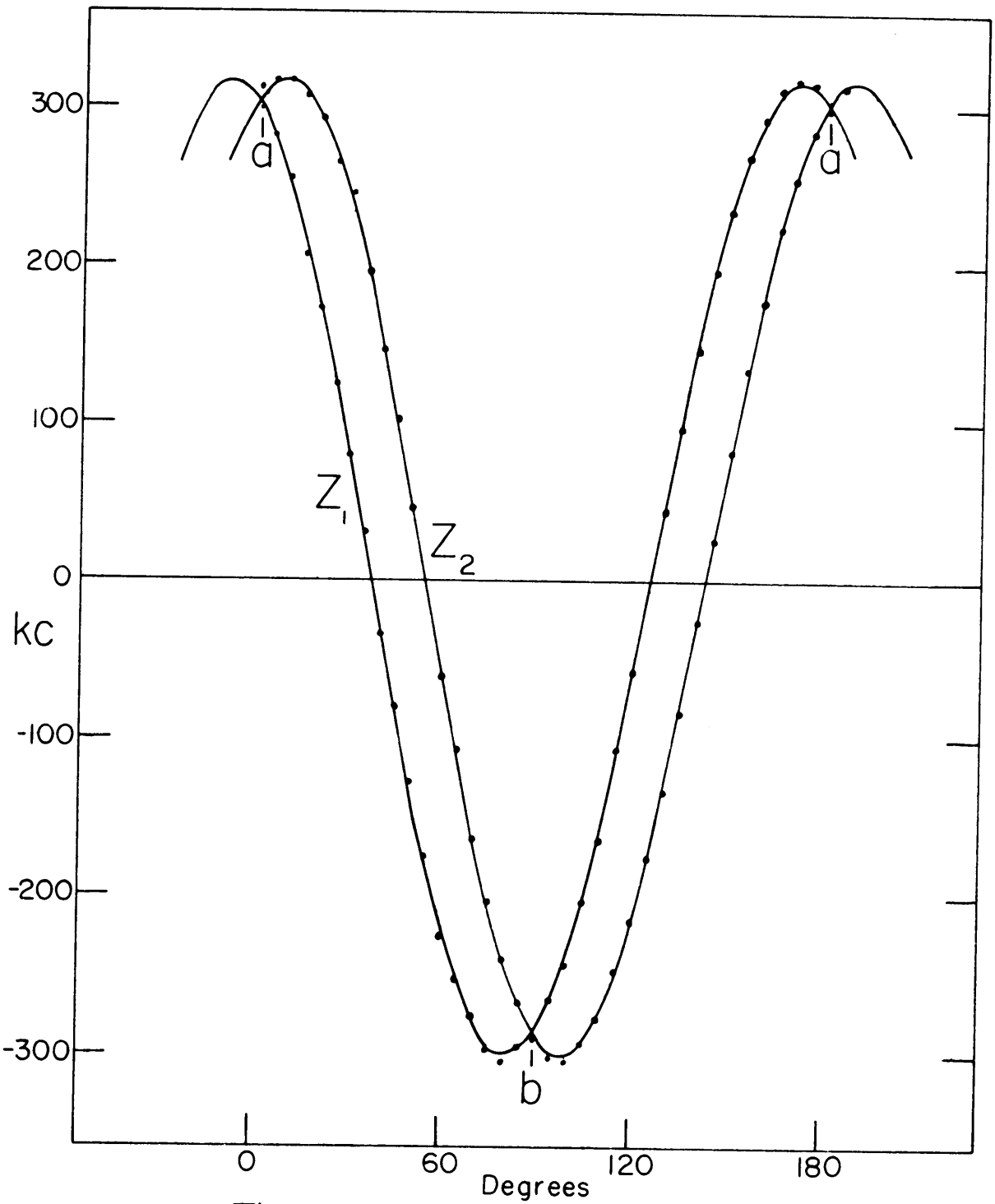

Figure X Z Rotation Graph

Frequency Interval Between Satellites Versus the Angle Between the X Axis and H_o

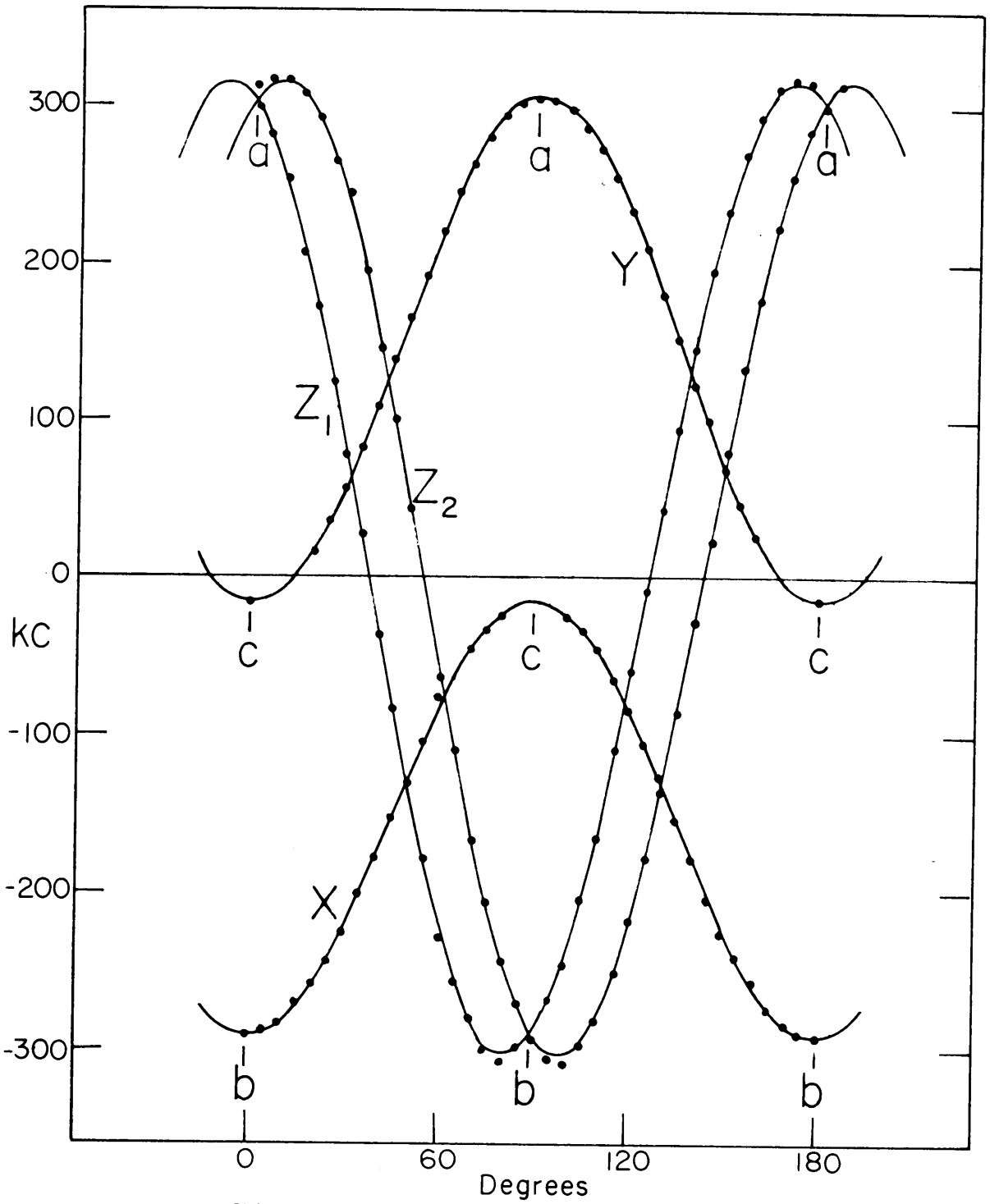

Figure XI XYZ Rotation Graph

Frequency Interval Between Satellites Versus the Angle Between the YZX Axes and H_0

$$2\Delta\nu = -152.4 - 138.8\cos 2\theta - .1846\sin 2\theta \quad (49)$$

or

$$= -152.4 - 138.8\cos 2(\theta + 0) \quad (50)$$

and for the Y or b rotation in Figure IX

$$2\Delta\nu = 145.2 - 160.8\cos 2\theta - 8.232\sin 2\theta \quad (51)$$

or

$$= 145.2 - 161.0\cos 2(\theta - 1.45^{\circ}) \quad (52)$$

For the Z or c rotation there are two curves, designated Z_1 and Z_2 in Figure X since two pairs of satellites are obtained. For Z_1 one obtains

$$2\Delta\nu = 8.232 + 293.8\cos 2\theta - 91.98\sin 2\theta \quad (53)$$

or

$$= 8.232 - 307.9\cos 2(\theta + 8.70^{\circ}) \quad (54)$$

and for Z_2

$$2\Delta\nu = 8.159 - 297.2\cos 2\theta + 87.27\sin 2\theta \quad (55)$$

or

$$= 8.159 + 309.8\cos 2(\theta - 8.18^{\circ}) \quad (56)$$

Both forms of Eq. (30) are displayed for each curve since the first form is more convenient for calculating the various matrix elements and the second more convenient for discussing the phase shifts. All coefficients are expressed in kc and are given to four significant numbers and the phase angles are given to the nearest hundredth of a degree. These are the coefficients from the least squares fit and the phase angles that are calculated from them. An accuracy of four significant numbers is not implied, for example note the constant C_X in Eq. (49). The zero in Eq. (50) is used only to imply that δ_X is zero to at least the nearest hundredth of a degree when it is calculated from the constants in Eq. (49).

The interpretation of the data is done by two different methods. In method one each of the curves in Figure X is grouped separately with the curves of Figures VIII and IX to determine the matrix elements of the field gradient tensors, since there are two different sites. The identities in Eq. (32) are used to obtain an average value for A_X and for B_X when the Z_1, X, and Y rotation curves are grouped together and then another average value for A_X and B_X when the Z_2, X, and Y rotation curves are grouped together. The constants from Eq. (49), (51), and (53) are substituted into Eq. (32) to obtain three equations that are each equal to A_X, namely

$$A_X = -152.4,\ (B_Y - A_Y)/2 = -153.0, \text{ and } -(B_Z + A_Z)/2 = -151.0$$

which give an average value for A_X of -152.1. Likewise one obtains for B_X the three equations

$$B_X = -138.8,\ -3(A_Y + B_Y)/2 = -137.4, \text{ and } (3A_Z - B_Z)/2 = -134.6$$

which gives an average value for B_X of -136.9.

The average values for A_X and B_X are now substituted into Eq. (31) to give

$$2A_X = K(\phi_{YY} + \phi_{ZZ}) = 2(-152.1),$$

$$2B_X = K(\phi_{YY} - \phi_{ZZ}) = 2(-136.9),$$

and

$$C_X = -K\phi_{YZ} = -.1846\ .$$

These equations and the trace condition yield

$K\phi_{XX} = 304.3$, $K\phi_{YY} = -289.1$,

$K\phi_{ZZ} = -15.20$, and $K\phi_{YZ} = .1846$.

From Eq. (31) and (53) one obtains

$$C_Z = - K\phi_{XY} = -91.98 ,$$

and from Eq. (31) and (51)

$$C_Y = -K\phi_{ZX} = -8.232 .$$

Thus one obtains for the matrix

$$\begin{pmatrix} 304.3 & 91.98 & 8.232 \\ 91.98 & -289.1 & .1846 \\ 8.232 & .1846 & -15.20 \end{pmatrix} \quad M_1 .$$

If one now combines the Z_2, X, and Y curves in the same manner one obtains

$$\begin{pmatrix} 305.4 & -87.28 & 8.232 \\ -87.28 & -290.2 & .1846 \\ 8.232 & .1846 & -15.20 \end{pmatrix} \quad M_2 .$$

In method two the interpretation is based on the arguments, as discussed in Section IIC, that the two different beryllium sites are at least equivalent sites and that the c axis is a principal axis of the electric field gradient. The two equations for the Z rotation curves should then be the same except that they are shifted right and left by equal angles from their points of intersection at zero and at 90 deg. Thus one averages the two values for C_Z from Eq. (53) and (55) and also averages each pair of diagonal

terms in M_1 and M_2. The argument that the c axis is parallel to a principal axis also allows one to use Eq. (45) which has four zero elements instead of Eq. (24). Thus one obtains the matrix

$$\begin{pmatrix} 304.9 & 89.62 & 0000 \\ 89.62 & -289.7 & 0000 \\ 0000 & 0000 & -15.20 \end{pmatrix} \qquad M_3$$

from this interpretation.

The equations in Section IIB that diagonalize the matrix were programmed for the computer. The program was written so that it gave the diagonalized matrix, the absolute value of the quadrupole coupling constant, the asymmetry parameter, the direction cosines, and the angles between the principal axes and the XYZ axes. The complete print-out from the computer for M_1 is as follows:

```
The original tensor is
      304.3000        91.9800         8.2320
       91.9800      -289.1000          .1846
        8.2320          .1846       -15.2000
The diagonalized tensor is
      -15.3961          .0000          .0000
         .0000      -303.0341          .0000
         .0000          .0000       318.4302
The direction cosines and angles are
Lamda  1=  .0236   Theta  1,X=  88.644 Degrees
   Mu  1=  .0072   Theta  1,Y=  89.583 Degrees
   Nu  1= -.9996   Theta  1,Z= 178.582 Degrees
Lamda  2= -.1497   Theta  2,X=  98.614 Degrees
   Mu  2=  .9887   Theta  2,Y=   8.617 Degrees
   Nu  2=  .0036   Theta  2,Z=  89.792 Degrees
Lamda  3=  .9884   Theta  3,X=   8.722 Degrees
   Mu  3=  .1496   Theta  3,Y=  81.392 Degrees
   Nu  3=  .0244   Theta  3,Z=  88.597 Degrees
Eta=   .9032
```

ABS. Value of the Quad. Coupl. Const.= 318.4302
a= 9.6732290E-04
b= 1.4856487E-06
Alpha= 27.5429 Degrees

Five of these angles should be zero, 90, or 180 deg when one of the principal axes coincides with one of the XYZ axes. Their average variation from these values is 1.0 deg. The other four angles should be either the phase angle δ_Z or 90 deg plus or minus the phase angle. The average value of these four phase angles is 8.6 deg. The matrix M_2 gives the same value for the asymmetry parameter, namely .9032, and a value of 318.1 kc for the absolute value of the quadrupole coupling constant. The corresponding angles are 1.0 deg for the average variation and 8.2 deg for the average phase angle.

In method two the simpler Eq. (47) and (48) are applied to M_3. These give .9044 for the asymmetry parameter, 318.1 kc for the quadrupole coupling constant and 8.4 deg for the phase angle, δ_Z.

B. Errors and Conclusions

It is difficult to estimate the error in the results. The experimental points and the curves obtained from the least squares fit show good agreement. The poorest agreement is with the Z rotation points and their curves. This is to be expected as the satellites are about half the size on these sweeps as they are on the sweeps for the X and Y rotations. This makes the determination of the centers of these satellites more difficult.

Several different arguments can be made concerning the angles. One is that in Eq. (52) the phase angle δ_Y is 1.45 deg when it should be zero as is δ_X in Eq. (50). Therefore the phase angles in Eq. (54) and (56) could contain the same error. Another argument is that the interpretation based on methods one and two both indicate a one degree error and an average value for δ_Z of 8.5 deg. Then the value for δ_Z, which is to be applied to both Eq. (52) and (54), will be stated as 8.5 ± 1 deg.

Similar arguments can be made for the absolute value of the quadrupole coupling constant and the asymmetry parameter. Their values will be stated as

$$\eta = .90 \pm .01 \text{ and } \left|\frac{e^2qQ}{h}\right| = 318 \pm 2 \text{ kc.}$$

There is no other known determination of these values. Schuster and Pake (13) used the fact that there were two

satellites for beryllium in chrysoberyl to verify that $I = 3/2$ for beryllium and also reported a splitting of as large as 480 kc, but no splitting of this magnitude was observed in this investigation. No explanation is suggested for this discrepancy. It is concluded that there are two different types of sites for the beryllium nuclei in chrysoberyl and that these sites are equivalent. The principal axis that corresponds to the smallest eigenvalue (15 ± 2kc) is parallel at both sites to the crystallographic c axis. The principal axis that corresponds to the intermediate eigenvalue (303±2kc) lies in the ab plane at both sites, but at one site it is rotated 8.5 ± 1 deg away from the b axis and at the other site it is rotated the same amount the opposite way from the b axis. The principal axes at the two sites that correspond to the largest eigenvalue (318 ± 2kc) likewise lie in the ab plane 8.5 ± 1 deg on opposite sides of the a axis.

V. ACKNOWLEDGEMENTS

The author wishes to express his appreciation to the following people for the reasons stated: Dr. T. E. Gilmer, Jr. for his help and interest in all phases of this investigation and all phases of the authors graduate program, Prof. W. Richardson and Dr. B. W. Nelson for their assistance with the crystal structure, , and for writing the computer programs and running the computer, for his assistance in the mechanical shop, . for his help with the various electronic problems, for making the drawings, and for the typing of this thesis.

VI. BIBLIOGRAPHY

1. Andrew, E. R., "Nuclear Magnetic Resonance", Cambridge University Press, London and New York, 1955.
2. Bloch, F., Hansen, W. W. and Packard, M. E., "Nuclear Induction". Physical Review Vol. 69, 1 and 15 January 1946, p. 127.
3. Bragg, W. L. and Brown, G. B., "Crystalline Structure of Chrysoberyl", Proceedings of the Royal Society of London Vol. 110, April 1926, p. 34.
4. Cohen, M. H. and Reif, F., "Quadrupole Effects in Nuclear Magnetic Resonance Studies of Solids", Solid State Physics Vol. 5, Academic Press Inc., New York, 1957.
5. Elmore, W. C. and Sands, M., "Electronics", National Nuclear Energy Series, McGraw-Hill Book Company, Inc., New York, 1949, p. 372.
6. Gutowsky, H. S., "Nuclear Magnetic Resonance", Annual Review of Physical Chemistry Vol. 5, 1954, p. 333.
7. Hoard, J. L., "Structures and Polymorphism in Elemental Boron", Advances in Chemistry Series Vol. 32, 1961, p.42.
8. Hockenberry, J. H., Brown, L. C. and Williams, D., "Nuclear Resonance Spectrum of Al^{27} in Chrysoberyl", The Journal of Chemical Physics Vol. 28, March 1958, p. 367.

9. Pake, G. E., "Nuclear Magnetic Resonance", Solid State Physics Vol. 2, Academic Press Inc., New York, 1956, p. 1.

10. Pound, R. V., "Nuclear Electric Quadrupole Interactions in Crystals", Physical Review Vol. 79, 15 August 1950, p. 685.

11. Purcell, E. M., Torrey, H. C. and Pound, R. V., "Resonance Absorption by Nuclear Magnetic Moments in a Solid", Physical Review Vol. 69, 1 and 15 January 1946, p. 37.

12. Ramsey, N. F., "Nuclear Moments", John Wiley and Sons, Inc., New York, 1953, p. 21.

13. Schuster, N. A. and Pake, G. E., "The Spin of Be^9", Physical Review Vol. 81, 1 March 1951, p. 886.

14. Sokolnikoff, I. S. and Redheffer, R. M., "Mathematics of Physics and Modern Engineering", McGraw-Hill Book Company, Inc. New York, 1958, p. 702.

15. Uspensky, J. V., "Theory of Equations", McGraw-Hill Book Company, Inc, New York, 1948. p. 92.

16. Varian Associates, "Twelve Inch Electromagnet System", Instrument Division Publication Number 87-150-005, Palo Alto, California, no date.

17. Volkoff, G. M., Petch, H.E. and Smellie, D.W.L., "Nuclear Electric Quadrupole Interaction in Single Crystals", Canadian Journal of Physics Vol. 30, May 1952, p. 270.

18. Wyckoff, R. W. G., "Crystal Structures", Vol. II, Interscience Publishers, Inc., New York, 1948-1957.

The vita has been removed from the scanned document

ABSTRACT

The quadrupole coupling constant ($|e^2qQ/h|$), the asymmetry parameter (η), and the orientation of the principal axes with respect to the crystallographic abc axes were determined for the sites of the beryllium nuclei in a single crystal of chrysoberyl.

Three single crystals of chrysoberyl were each in turn rotated about a different crystallographic axis in a constant magnetic field of approximately 12,000 gauss. The interaction of the electric field gradient at the Be^9 site and the electric quadrupole moment of the beryllium nucleus ($I=3/2$) produces a frequency spectrum consisting of a central resonance and two satellites on either side of the central line for each unique beryllium site. The frequency interval between the two satellites depends on the particular crystal orientation in the constant magnetic field. This frequency interval was measured for various crystal positions in each of the three crystal rotations. A nuclear magnetic resonance spectrometer, employing a Collins type marginal oscillator and a 12 inch electromagnet, was used to determine these frequency intervals.

The experimental points consisting of the frequency intervals versus the angular positions of the crystal for each pair of satellites were fitted to the theoretical curve

that is predicted from a first order pertubation treatment of the quadrupole interaction on the magnetic energy levels. The Volkoff Method of rotation analysis was then used to relate the fitted constants in the above equations to the elements of the electric field gradient tensor and to obtain the diagonalized form of this tensor. The diagonal elements of this tensor then gave immediately the value of η and $|e^2qQ/h|$. These values were found to be as follows:

$$\eta = .90 \pm .01 \quad \text{and} \quad |e^2qQ/h| = 318 \pm 2 \text{ kc.}$$

The rotation about the c crystal axis showed two pairs of satellites of nearly equal strength which indicated two different types of sites for the beryllium nuclei. The three eigenvalues for one site were found to have the same value as the same three eigenvalues for the other site. Thus the two sites have the same field gradient components but the orientations of the two sites are different. The crystal symmetry of chrysoberyl predicts that one of the principal axes should be parallel to the c crystal axis. The principal axes at the two sites that correspond to the smallest eigenvalue of the diagonalized tensor (15.2 $\pm$ 2kc) were found to be parallel to the c axis. The principal axes at the two sites that correspond to the largest eigenvalue (318 $\pm$ 2kc) lie 8.5 $\pm$ 1 deg on either side of the a crystal axes in the ab plane. The principal axes that correspond

to the intermediate eigenvalue (303 ± 2kc) lie 8.5 ± 1 deg on either side of the b axes in the ab plane.